Nonthermalized excited states in Ru(II) polypyridyl complexes probed by ultrafast transient absorption spectroscopy with high photon energy excitation

Sherri A. McFarland, Karen A.W.Y. Cheng, Felix S. Lee, Frances L. Cozens, and Norman P. Schepp

Abstract: The picosecond excited state dynamics of a series of homoleptic Ru(II) polypyridyl complexes (where LL = bpy, dmb, dmeob, dfmb, or dttb) have been investigated in aqueous solution at room temperature using femtosecond transient absorption spectroscopy with high photon energy excitation. All of the complexes studied produced similar spectroscopic signatures: a near-instantaneous bleach centered at 470–500 nm corresponding to the static absorption spectrum, as well as an intense absorption (475–650 nm) that decayed within the instrument response function (IRF) to form a broad, low-level absorption extending from 500–650 nm. Detailed analyses of both kinetic and spectral parameters by singular value decomposition (SVD) indicate that the excited state difference spectra contain contributions from at least three distinguishable species that have been assigned as ligand-based $\pi^* \leftarrow \pi^*$ and ligand-to-metal-charge-transfer (LMCT) transitions concomitant with the loss of the ground state metal-to-ligand-charge-transfer (MLCT) transition. Kinetic information extracted at 530 nm (an optical marker for the fully intraligand-delocalized ^{3}MLCT state) or 660 nm (LMCT transitions) appear to be biphasic in some cases with the amplitude of the IRF-limited component becoming larger with shorter wavelength excitation. Further, rise dynamics were observed at redder probe wavelengths for $Ru(bpy)_3^{2+}$ and $Ru(dttb)_3^{2+}$. These observations are different from those obtained using lower photon energy excitation and show that excitation wavelength strongly influences the early photophysical events in these Ru(II) complexes.

Key words: ruthenium, photophysics, lasers, transient absorption spectroscopy, excited states, singular value decomposition (SVD).

Résumé : Opérant à la température ambiante, en solution aqueuse, et faisant appel à la spectroscopie d'absorption des états transitoires au niveau de la femtoseconde et une excitation à l'aide de protons de haute énergie, on a étudié la dynamique d'états excités à la picoseconde d'une série de complexes polypyridyles du ruthénium(II) homoleptiques [dans lesquels LL = bpy, dmb, dmeob, dfmb ou dttb). Tous les complexes étudiés produisent des signatures spectroscopiques semblables: une décoloration pratiquement instantanée centrée aux environs de 470 à 500 nm correspondant au spectre d'absorption statique ainsi qu'une absorption intense (475–650 nm) qui décroît en dedans de la fonction de réponse de l'instrument (FRI) pour former une large absorption de faible intensité s'étendant de 500 à 650 nm. Des analyses détaillées des paramètres tant cinétiques que spectraux par la méthode de décomposition de valeur singulière (DVS) indique que le spectre différentiel de l'état excité contient des contributions provenant d'au moins trois espèces distinctes qui ont été attribuées à des transitions $\pi^* \leftarrow \pi^*$ à base de ligand et d'autres de transfert de charge ligand à métal (TCLM) concomitantes avec la perte de la transition de transfert de charge métal à ligand de l'état fondamental (TCML). L'information cinétique extraite des bandes à 530 nm (un marqueur optique pour l'état TCML) ou 660 nm (transitions TCLM) semble être biphasique dans certains cas, alors que l'amplitude de la composante limitée par la fonction de réponse de l'instrument devient plus importante lorsque la longueur d'onde de l'excitation devient plus courte. De plus, avec les complexes $Ru(bpy)_3^{2+}$ et $Ru(dttb)_3^{2+}$, on a observé une augmentation de la dynamique aux longueurs d'onde plus rouges de la sonde. Ces observations sont différentes de celles obtenues à l'aide d'une excitation avec des photons de plus faible énergie et elles démontrent que la longueur d'onde de l'excitation influence fortement les premiers événements photophysiques dans ces complexes du Ru(II).

Mots-clés : ruthénium, photophysique, lasers, spectroscopie d'absorption des espèces transitoires, états excités, DVS.

[Traduit par la Rédaction]

Received 8 June 2008. Accepted 18 September 2008. Published on the NRC Research Press Web site at canjchem.nrc.ca on 19 November 2008.

S.A. McFarland.[1] Chemistry Department, Acadia University, Wolfville, NS B4P 2R6, Canada.
K.A.W.Y. Chen, F.S. Lee, F.L. Cozens, and N.P. Schepp. Department of Chemistry, Dalhousie University, Halifax, NS B3H 4J3, Canada.

[1]Corresponding author (e-mail: sherri.mcfarland@acadiau.ca).

 doi:10.1139/V08-161

Fig. 1. (*a*) Jablønski diagram showing the well-established photophysical model for the tris-Ru(II) polypyridyl family of complexes; (*b*) Jablønski diagram illustrating the photophysics of $Ru(dmb)_3^{2+}$ derived from transient absorption experiments; (*c*) Jablønski diagram showing the nonthermalized excited-state dynamics of $Ru(bpy)_3^{2+}$ based on fluorescence upconversion experiments.

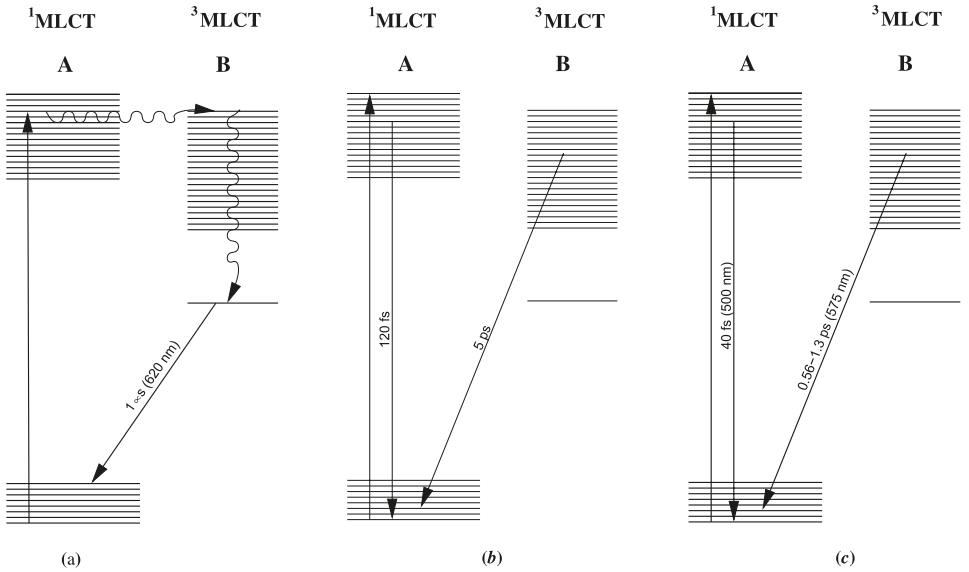

Introduction

A growing area of research involves the systematic investigation of photochemical and photophysical properties that define the behaviour of both organic and inorganic systems on short timescales. These endeavours not only provide invaluable information regarding the electronic structure of molecules, they also further our ability to use rational design in the construction of light-dependent molecular devices (1–4). Such an approach to functional chromophores requires a fundamental understanding of how molecules absorb and dissipate radiant energy. Often, absorption of photonic energy does not directly populate the lowest-lying electronic state of a molecule, the state that is usually involved in photon emission or photochemical reactions on conventional timescales. In fact, a host of states may be sampled between initial population of the Franck–Condon state and relaxation over all electronic and vibrational modes in the excited manifold, invoking a variety of radiationless decay mechanisms. Internal conversion (IC), intersystem crossing (ISC), and vibrational relaxation (VR) are important decay channels that ultimately dictate the path of excited state evolution and influence emission quantum yields as well as spectra.

The unifying feature of nonradiative decay among excited states is the short time that it takes for these transitions to occur. With the advent of femtosecond lasers, elucidation of ultrafast dynamics in both organic and inorganic systems is now possible, and reports from a number of groups studying diverse chemical systems continue to outline the importance of the earliest stages of excited state evolution (5–10). For example, nonthermalized excited states have been implicated in a variety of processes from electron and energy transfer (11, 12) to photochemical reactions including isomerization and ligand dissociation (13, 14). Perhaps more notable is the role that higher excited states play in applications involving solar energy conversion (15). Specifically, work from numerous laboratories has shown that the use of transition metal complexes as sensitizers for wide-band gap semiconductors is dependent on the efficiency of electron injection from the dye to the TiO_2 conduction band (16). This efficiency is determined by two competing processes: interfacial electron transfer and intramolecular relaxation dynamics (17, 18). Evidence suggests that electron transfer rates are maximal when operating in the nonergodic regime (19, 20)[2]; therefore, detailed investigation of the processes that immediately follow photon absorption is critical for developing more efficient devices based on this technology.

Nonradiative transitions among excited states are determined by the relative rates of electronic surface crossings and vibrational relaxation. Established models of intramolecular excited state relaxation are based largely on simple cascade population dynamics observed for organic molecules, wherein vibrational relaxation is much faster than formal changes in electron spin multiplicity ($k_{vib} \gg k_{IC} \gg k_{ISC}$) (21). Systems characterized by a large number of electronic and vibrational states that can participate in excited state decay do not adhere to this simplified kinetic scheme; consequently, excited state decay in transition metal complexes ultimately depends on the state(s) initially populated, resulting in a strong excitation-wavelength dependence of the observed kinetics, as well as ISC rates that are much faster than VR (9, 14, 22).

For example, both transient absorption and fluorescence upconversion experiments indicate that ISC in $Ru(bpy)_3^{2+}$ occurs with a time constant of $\tau = 40 \pm 15$ fs, whereas vibrational cooling in the ^{3}MLCT manifold spans several picoseconds when pumped at 400 nm (5, 23). Longer wavelength excitation ($\lambda_{ex} = 480$ nm) produces no significant changes in the excited state absorption spectra beyond 300 fs; these subpicosecond dynamics are reported to encompass a host of

[2] The term *nonergodic* in this context is used to describe a state that has not thermally equilibrated on the excited state surface. These states are intermediate in energy between the Franck–Condon state(s) and the Boltzmann-distributed ^{3}MLCT state(s).

Fig. 2. Jabløonski diagram illustrating the nonthermalized excited state dynamics for $Ru(dmb)_3^{2+}$ modified to include τ_2.

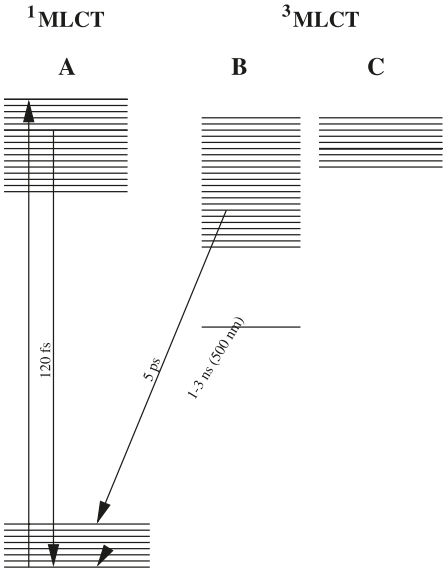

processes including ISC, IC, charge localization, VR, and intramolecular vibrational energy redistribution (IVR). Figure 1 summarizes these recent modifications to the well-established photophysical model for ruthenium(II) polypyridyl complexes.

To elucidate further the early events following photon absorption by transition metal complexes, our group has documented the picosecond dynamics produced in response to population of nonthermalized excited states in $Ru(bpy)_3^{2+}$ and a series of its derivatives by high photon energy excitation (24). Pump wavelengths of 388 and 258 nm produce emission at 500 nm that is more complex than previously reported using longer wavelength excitation (5, 6). Specifically, we determined additional time constants of τ = 1–3 ns for a series of 4,4′-substituted ruthenium(II) bipyridyl complexes (Fig. 2); while this additional relaxation pathway was not observed for $Ru(bpy)_3^{2+}$ with 388 nm excitation, 258 nm excitation of $Ru(bpy)_3^{2+}$ gave rise to a small contribution from the longer-lived component. These findings demonstrate the need for a comprehensive reassessment of our current understanding of inorganic photophysics, with an appreciation for the information that can be gleaned from close examination of the excitation-wavelength dependence of the observed kinetics.

Recently, our research efforts have concentrated on the use of picosecond luminescence and femtosecond absorption spectroscopy to address the excitation-wavelength dependence of excited state evolution in $Ru(bpy)_3^{2+}$ and related derivatives. In particular, we used femtosecond absorption spectroscopy to investigate the nature of a longer-lived state (τ = 1–3 ns) that was first detected in our earlier work involving picosecond luminescence experiments with short-wavelength excitation. We note a significant contribution to excited state decay from a broad band in the visible region that decays within the instrument response function (IRF) when pumped with 388 nm excitation. While the resolution of our instrument precluded the accurate determination of rate constants for the various processes, we were able to use

Chart 1. Bipyridyl ligands studied using transient absorption spectroscopy with 388 nm excitation.

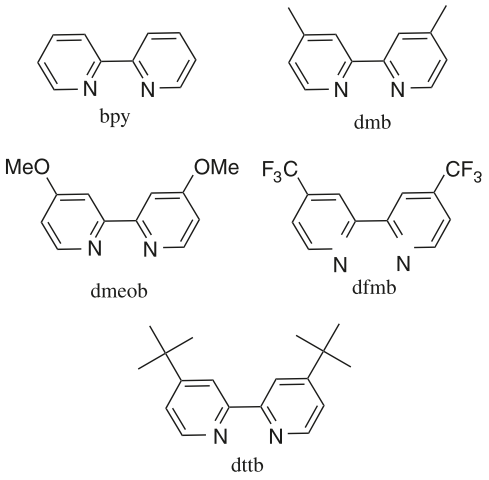

singular value decomposition (SVD) to discern rise dynamics that have not been previously reported for several of the complexes. Through this work we show that both excitation wavelength and subtle changes in ligand identity influence the nature of excited state dynamics, a finding of significant importance in the field of optoelectronic device construction. Moreover, these findings further support the observation that simple cascade population dynamics are not sufficient to describe the photophysics of transition metal complexes, and a growing number of exceptions for organic molecules have been documented as well (25–27).

Experimental section

Materials

Ruthenium(II) complexes (Cl_2 and $(PF_6)_2$ salts) and their corresponding ligands (Chart 1) were synthesized according to modified literature protocols (24) and chromatographed on silica gel ($MeCON:H_2O:KNO_3$ gradient) or on Sephadex. Following recrystallization from an acetonitrile/toluene mixture, the complexes were characterized by TLC, ^1H NMR, ^{13}C NMR, HPLC, and mass spectrometry. HPLC traces were run on samples before and after laser irradiation to ensure sample degradation was not a factor in the transient absorption experiments.

Static and nanosecond time-resolved spectroscopies

Static absorption, emission, and nanosecond time-resolved emission measurements were carried out as previously described (24), and where possible, the parameters obtained from static and nanosecond spectroscopies were compared with those in the literature.

Picosecond time-resolved emission spectroscopy

Time-resolved luminescence measurements were performed using a Clark-MXR CPA-2001 femtosecond laser for sample excitation and a streak camera (Axis-Photonique) coupled to a CCD camera (SenSys) for detection. Experimental details are reported elsewhere (24).

Sample preparation for femtosecond absorption spectroscopy

Ruthenium(II) complex (50 mL, 1 mmol/L) was diluted with solvent until the absorbance of the solution was 0.4–0.6 at 388 nm. This solution was recycled at a flow rate of 116.5 mL/min by a varistaltic pump through a Helma quartz flow cell (1 mm). The collection process was randomized to eliminate effects due to systematic sample degradation. Each raw spectrum consisted of 2500 accumulated shots and was corrected for luminescence and dark counts. Three of these raw spectra were averaged to produce the experimental spectrum recorded; each raw spectrum was manually inspected to discount faulty shots due to laser instability.

Femtosecond transient absorption spectroscopy

Femtosecond electronic absorption data were acquired using a Clark-MXR CPA-2001 femtosecond laser for generating pump and probe beams and a SpectroPro-300i Imaging spectrograph (Acton Research Corporation) equipped with an ST-116 photodiode array (PDA, Princeton Instruments, Inc.) for detection. Briefly, the CPA-2001 employs an all solid-state diode-pumped Erbium-fiber laser, which generates <150 fs, 775 nm pulses at 1 KHz with an output energy of ~800 μJ per pulse. The output is split by a STORC-2001 unit (Clark-MXR); one of the pulses is frequency-doubled to 388 nm (or tripled to 258 nm) to produce the pump beam, and the unchanged fundamental is used to generate a white-light continuum in sapphire (1 mm) or water contained in a 30 mm quartz cell. The frequency-doubled 388 nm pump beam (216 fs, 7 mm in diameter) is directed to the sample using a series of thin film mirrors and is softly focused (~1.5 mm) on the sample cell 15° from normal through a plano-convex lens with a 50 mm focal length. The excitation power at the sample is ~3.5 μJ, and for the series of complexes studied, the signal response varies linearly as the power is attenuated.

The 775 nm light used to generate the white light continuum is directed by a series of thin-film mirrors through two variable delay rails: the Parker Rail Table (Parker) allows time delays up to 7 ns with 188.3 fs resolution, while the NanoStepper (Baldor Motion Products) allows the probing of the first 500 fs of the experiment with 33.36 fs resolution. Once the fundamental beam passes through the second delay rail, it is directed through a Berek's compensator (New Focus), with the alignment and retardance set to emulate a 1/2 wavelength waveplate for 775 nm radiation, and a Glan-laser polarizer (Thorlabs). The Berek's compensator and Glan-laser polarizer together form a variable attenuator with output polarized at 54.7° with respect to the pump beam to avoid anisotropy effects. The polarized pump beam is focused by a 100 mm focal length BK7 broadband antireflective (BBAR)-coated planoconvex lens into a white light generator, and the broadband radiation is collimated by an achromatic MgF_2 lens with a focal length of 50.8 mm. If a water cell is used as the white light source, a Schott colour glass filter (S8612) is inserted to attenuate selectively the red wavelengths, and an iris is present to isolate the stable center of the broadband beam. Finally, the probe beam is focused (0.2 mm diameter) using an achromatic lens (150 mm focal length) through the sample onto a fibre optic cable.

Fig. 3. Potential energy surface diagram depicting the influence of excitation energy on population dynamics.

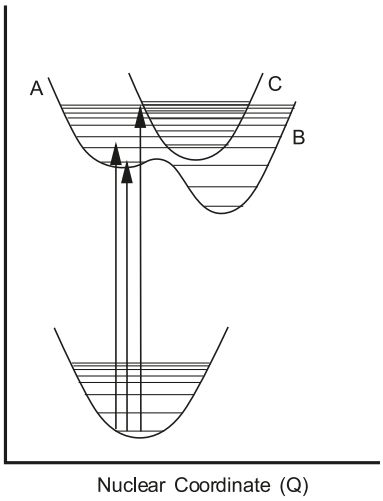

To collect full-spectrum data, the fibre optic cable directs transmitted light from the sample into a SpectroPro-300i Imaging spectrograph (Acton Research Corporation) coupled to a thermoelectrically cooled ST-116 PDA detector (Princeton Instruments, Inc.). A standard general purpose information bus (GPIB) computer interface allows data to be accumulated on a chip to maximize the number of laser experiments that can be measured while minimizing data transfer time. Absorbance values were calculated at each wavelength according to the following equation

$$A = \log\left(\frac{C_{\text{probe}} - D}{R_{\text{pump probe}} - F_{\text{pump}}}\right)$$

where A is the calculated absorbance value, C_{probe} is the probe data in the absence of the pump beam, D represents the dark counts, $R_{\text{pump,probe}}$ is the probe data collected while the pump beam is incident on the sample cell, and F_{pump} is the fluorescence data collected with the pump beam only. Since the chirp in our probe beam is significant over the spectral window (450–750 nm), distortion of the spectra at early times must be corrected. Unchirped spectra were produced from the original data using software written in-house. The temporal-spectral profile of the chirped pulse, a parameter required by the program, was calculated from two-photon absorption spectra of 2-methylnathphalene. Once $t = f(\lambda)$ has been determined, it remains invariant as long as the experimental setup is not altered.

Singular value decomposition

SVD analysis was carried out on the unchirped absorption spectra using MATLAB®. New matrices were constructed from the best three-component representations of the original, unchirped transient matrix spectra. Kinetics were then compared for the original data matrices and the results of the SVD at every 100th wavelength. Wavelength indices were selected to interrogate regions of the spectra corresponding to MLCT and LMCT transitions (480, 532, and 650 nm) and to determine the utility of SVD as a noise filter for address-

ing limitations imposed by the resolution of our current laser setup.

Results and discussion

Figure 3 provides a model illustrating the effect of excitation wavelength on the state(s) initially populated for some ruthenium(II) polypyridyl complexes. This qualitative picture is based on our recent discovery that 388 nm excitation produces picosecond luminescence at 500 nm that is not observed in experiments carried out with longer wavelength excitation (24). Femtosecond transient absorption spectra collected after 480 nm excitation as well as 400 nm excitation further corroborate this model (5, 6). The general trend is toward simpler kinetics when longer wavelength excitation is used, suggesting that less energetic wavelengths preclude access to some states. Our modification of the original kinetic model outlined by Bhasikuttan et al. (23) for $Ru(bpy)_3^{2+}$ (Fig. 2) proposes that state A represents the ^{1}MLCT manifold and state B represents the corresponding triplet manifold; the nature of state C, emissive only when high photon energy excitation is used, is the subject of this investigation.

We previously outlined three plausible scenarios concerning the nature of state C: (*i*) a higher vibrational level of state B, (*ii*) a local minimum on the surface of state B, or (*iii*) a distinct state altogether (24). If state C were indeed a "hot" vibrational state of B, then its lifetime would be expected to be much shorter than the observed lifetime (τ = 1–3 ns) since vibrational cooling is generally on the order of 0.5–5 ps. Therefore, only the latter possibilities need to be considered. To distinguish among these possibilities, we used femtosecond transient absorption spectroscopy to probe picosecond and subpicosecond dynamics.

Full-spectrum transient absorption data for all five ruthenium(II) homoleptic complexes (based on the ligands shown in Chart 1)[3] contained several unifying spectral features that were evident regardless of the timescale of the experiment (Figs. S1–S6).[4] Excitation at 388 nm produced the characteristic ^{1}MLCT ground state bleach centered in the range of 450–500 nm with maxima determined by the identity of the ligand substituents, which was superimposed on a broad absorption band spanning 475–650 nm. This extended absorption region consisted of two overlapping absorption bands as determined by spectroelectrochemical measurements: absorption transitions due to the reduced ligand at 500–530 nm and LMCT transitions involving the oxidized ruthenium center at 575–665 nm. These data agree well with spectra reported in the literature utilizing longer pump wavelengths (5, 6). However, the kinetics and relative amplitudes associated with these transitions exhibit an excitation-wavelength dependence not reported previously. Further, to our knowledge, the ultrafast dynamics of homoleptic 4,4′-methoxy, -trifluoromethyl, and -*tert*-butyl Ru(II) polypyridyl complexes have not been reported.

Upon excitation at 388 nm, all of the ruthenium(II) homoleptic complexes investigated produced spectroscopic signatures that remained unchanged when probed in 100 ps intervals from –0.5 ps to 5 ns. Considering the pronounced decay (τ = 1–3 ns) observed at 500 nm for the homoleptic 4,4′-substituted bipyridyl complexes in the luminescence experiments (τ_{ex} = 388 nm) and the absence of discernible decay kinetics in the region interrogating reduced bipyridine ligands in the corresponding transient absorption experiments, we conclude that the absorptive properties we observe are indicative of triplet surface dynamics.[5] The characteristic spectroscopic signatures, as well as established timescales for the formation of the ^{3}MLCT state (5, 6, 23) are consistent with such a conclusion. Based on the assumption that distinct states will produce distinct spectral characteristics, we assign state C as a metastable entity of ^{3}MLCT origin (scenario (*ii*), vide supra) that is accessed only with relatively short-wavelength excitation. Both steric and electronic perturbation of the complexes, by variation in ligand identity, produced similar results, indicating that this state is a general feature of homoleptic ruthenium(II) 4,4′-substituted bipyridyl complexes when probed with short-wavelength excitation. At even shorter wavelength excitation (τ_{ex} = 258 nm), similar states in the parent $Ru(bpy)_3^{2+}$ are populated (24). It should be noted that there is no reason a priori to expect that a decay in emission measurements should have a corresponding transient in the absorption measurements: the transitions being probed are not the same. Moreover, uncertainty exists with regard to whether the transients are actually absent in the absorption data as the absorption spectra are complicated by a superposition of MLCT and LMCT transitions that may mask any pertinent kinetics associated with the transition of interest.

Transient absorption spectra were also collected for all five homoleptic complexes on shorter timescales (*t* = 0–15 ps). Excitation with 388 nm radiation in aqueous solutions produced bleach signals corresponding to the ground

[3] The ultrafast dynamics of $Ru(bpy)_3^{2+}$ have been studied previously by fluorescence upconversion as well as transient absorption spectroscopy using longer pump wavelengths. $Ru(dmb)_3^{2+}$ has been studied previously by transient absorption spectroscopy with longer pump wavelengths. To the authors' knowledge, the nonthermalized excited states for homoleptic complexes derived from dmeob, dfmb, and dttb have not been reported previously.

[4] Supplementary data for this article are available on the journal Web site (canjchem.nrc.ca) or may be purchased from the Depository of Unpublished Data, Document Delivery, CISTI, National Research Council Canada, Ottawa, ON K1A 0R6, Canada. DUD 3850. For more information on obtaining material refer to cisti-icist.nrc-cnrc.gc.ca/cms/unpub_e.shtml.

[5] It should be noted that the luminescence we observed in the picosecond experiments at 500 nm occurred with a quantum yield having an upper limit of ~10^{-4}, estimated by the absence of 500 nm emission when using a conventional steady-state fluorimeter. If one assumes that this low quantum yield represents a rather small portion of the initially excited molecules, then corresponding changes in the transient absorption spectrum may not be detectable unless there is an allowed transition with appreciable oscillator strength from this weakly luminescent state. In the absence of significant changes in the spectroscopic profile of the complexes when probed with shorter wavelength excitation, we assume dynamics reflect relaxation in the triplet manifold. Similarly, we assume that the absence of dynamics in the transient absorption spectra indicates no signicant change in electronic configuration of the weakly luminescent state relative to the triplet state formed by ISC with a time constant of 40 fs. This assumption should be constantly re-examined for each particular case.

Fig. 4. Transient absorption spectra for $Ru(dmb)_3^{2+}$ in aqueous solution following <150 fs excitation at 388 nm.

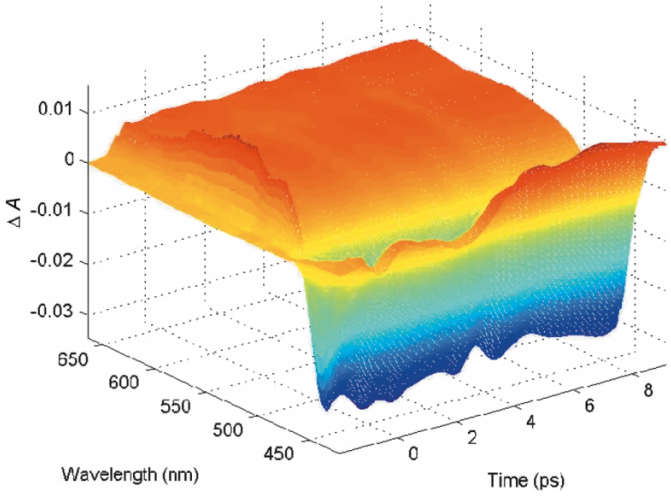

state ^{1}MLCT absorption, with precise maxima determined by the identity of the ligand (Fig. 4). Interestingly, the loss of ground state population did not appear instantaneous due to an overlapping broad absorption band that extended into the bleach region. This intense signal decayed within the instrument response function (~305 fs) to form a broad, low-level absorption extending from 500 to 650 nm that was identical to the absorption signature observed at 5 ns. After 1 ps, each absorption spectrum was relatively constant out to 15 ps in regions representative of the ground state bleach and bipyridine radical anions, a finding that contrasts with what others have measured for $[Ru(dmb)_3](PF_6)_2$ in acetonitrile resulting from 400 nm (~120 fs) excitation (6).

Previous femtosecond electronic absorption spectroscopy on $[Ru(dmb)_3](PF_6)_2$ reveals biexponential kinetics, which are not complete until ~15 ps at 532 nm. This portion of the spectrum is characteristic of the dmb^- chromophore (6). Deconvolution reveals a fast component ($\tau = 120 \pm 40$ fs) reported to reflect contributions from the ^{1}MLCT $\rightarrow$ ^{3}MLCT surface crossing on the timescale of the excitation pulse as well as a slower decay ($\tau = 5 \pm 0.5$ ps) due to vibrational cooling dynamics in the ^{3}MLCT excited state. With 388 nm (~150 fs) excitation, the slower dynamics previously associated with vibrational cooling in the triplet manifold are virtually absent and the signal is dominated by a transient that decays within the excitation pulse. In the absence of major changes in the overall spectroscopic signature for $[Ru(dmb)_3](PF_6)_2$ when excited with higher photon energy, we tentatively conclude that vibrational cooling is further facilitated when the Frank–Condon state possesses excess energy. The guiding principle in this assumption is that a constant spectral profile as a function of time indicates that the observed kinetics are not associated with a significant change in the electronic structure of the molecule (9). However, the excitation wavelength determines the nature of the initially populated vibronic hot state (16), and it is possible that the state initially populated could be fundamentally different, e.g., an intraconfigurational transition that does not significantly perturb the excited state absorption spectrum. Femtosecond infrared measurements will prove useful in future investigations regarding the dynamics associated with IVR and VC in these complexes.

Another interesting point of difference, with respect to the dynamics of $[Ru(dmb)_3](PF_6)_2$ when the pump wavelength is shortened, occurs in regions representative of predominantly LMCT transitions. With 388 nm excitation, we observed a sharp decay within the IRF superimposed on a low-level absorption that was constant out to 15 ps. According to Damrauer and McCusker (6), excitation (~120 fs) at 400 nm produces no discernible dynamics at 650 nm. Since spectroelectrochemical measurements indicate that there are contributions from both LMCT and dmb^- absorptions of the excited state, it is possible that this time-independent data at 650 nm reflect a superposition of decay and rise kinetics associated with two distinct signals that occur in a similar wavelength regime. In a case where a single process dictates evolution dynamics, time-independent data at 650 nm indicate that the dynamics must be highly localized, representing only the ligand housing the π^* electron of the ^{3}MLCT state. Our observation of a very fast decay in this region corroborates the assertion that the lack of dynamic features at 650 nm ($\lambda_{ex} = 400$ nm) in previous studies (6) is due to a superposition of LMCT and dmb^- absorptions, i.e., both the oxidized ruthenium center as well as a neutral ligand also contribute to the early events following photon absorption. Further, changing the excitation wavelength by only 12 nm changes the relative contributions of LMCT and dmb^- decay channels. Not only is this observation interesting from a photophysical standpoint, such control over excited state processes in transition metal complexes underscores the idea that judicious selection of excitation wavelength can profoundly influence the nature of excited state decay and may prove useful in tuning sensitizer properties for light-mediated applications.

To quantify time constants associated with the dynamics observed with 388 nm excitation of the complexes, we attempted to apply the method of singular value decomposition (SVD). SVD has been used successfully by others to analyze μs–fs transient absorption spectra when two or more transient species are involved (28–32). Briefly, a set of time-resolved spectra can be treated as a matrix **A**, where the *i*th row vector corresponds to the spectrum at the *i*th time delay point. According to the SVD theorem, the $m \times n$ $\Delta\mathbf{A}$ matrix can be written as the product of three matrices

$$\Delta\mathbf{A} = \mathbf{U}\cdot\mathbf{S}\cdot\mathbf{V}^T$$

where $\Delta\mathbf{A}$ is a $m \times n$ matrix consisting of absorbance changes at m wavelengths and n different time delays, **U** is a $m \times n$ matrix consisting of n orthonormal basis spectra, **S** is a $n \times n$ diagonal matrix containing the positive square roots of the eigenvectors (singular values) of **A**, and **V** is a $n \times n$ matrix where the columns (rows of $\mathbf{V}^T$) contain the time course amplitude for the corresponding basis spectra in matrix **U**. Basis spectra are scaled by their singular values to display their relative contributions to the observed data. The most useful information is contained in the first few components; increasing noise in the successive components results from the decreased amplitude of each basis spectrum in the observed spectra.

The SVD of the set of time-resolved spectra yielded four principal singular values (for all of the complexes) with $n =$

5 and higher singular values being almost zero and regarded as noise. Figure 4 was derived from the best four-component representation of the data matrix, illustrating the use of SVD as a noise filter (see Fig. S1 for original matrix).[4] Our attempts to use SVD as well as global analysis to extract kinetics did not yield readily interpretable results. This was not surprising given the lack of significant changes in the overall spectral profiles associated with relaxation processes such as vibrational cooling. A major problem with ultrafast dynamics is that nonthermalized excited states give rise to spectra that evolve continuously over time, precluding access to well-defined spectra.

Although the use of SVD and global analysis to extract time constants met with little success, the techniques did prove useful in analyzing the behaviour of the homoleptic complexes at long probe wavelengths, in the region dominated by LMCT transitions superimposed on the low energy shoulder of the reduced ligand $\pi^* \leftarrow \pi^*$ absorption. For both $Ru(dfmb)_3^{2+}$ and $Ru(dmb)_3^{2+}$, an IRF-limited decay to a constant background was observed. In the case of $Ru(dmb)_3^{2+}$, the absorption profile as a function of time with 388 nm excitation was very similar to that observed with longer excitation wavelengths (6), with the exception that the relative amplitude of the fast component to constant background was much larger with shorter wavelength excitation. This increased amplitude for the IRF-limited component with 388 nm excitation was a general feature that we observed for all of the complexes in regions probing both $\pi^* \leftarrow \pi^*$ and LMCT transitions. As indicated earlier, we are uncertain whether an increase in the rate of vibrational relaxation or a fundamental difference in the nature of the excited state(s) being probed is responsible; variable wavelength excitation should help clarify. These fast decay dynamics are difficult to interpret but are expected to reflect contributions from the ^{1}MLCT $\rightarrow$ ^{3}MLCT surface crossing. The absence of slower dynamics at 660 nm was not surprising given that λ_{probe} = 532 nm produced only an IRF-limited decay.

$Ru(bpy)_3^{2+}$ and $Ru(dttb)_3^{2+}$ showed interesting behaviour, as indicated in Fig. 5, for $Ru(dttb)_3^{2+}$. An IRF-limited decay followed by a slower rise that did not maximize over the observation window were noted in the transient absorption experiments collected over 15 ps. The slow rise must reach an asymptote shortly after 20 ps, however, since no changes were detected in this region in spectra collected over –0.5–5 ns. To our knowledge, this behaviour has not been documented for $Ru(bpy)_3^{2+}$ when excited at longer wavelengths, and this is the first report on the early dynamics of $Ru(dttb)_3^{2+}$. Curiously, λ_{probe} = 532 nm did not reveal similar rise kinetics, although others have observed analogous discrepancies for $Ru(dmb)_3^{2+}$ (6). In the case of $Ru(dmb)_3^{2+}$ excited at longer wavelengths, a slow decay is observed at λ_{probe} = 532 nm with no corresponding transient at λ_{probe} = 650 nm. The rationale behind this inconsistency, as well as others, has been attributed to an increase in the rate of vibrational cooling as the excited state(s) are probed farther to the red (6, 33, 34). Clearly, this particular explanation does not account for our observations for $Ru(dttb)_3^{2+}$ with shorter wavelength excitation and, therefore, should not be considered a general rule. Perhaps, in this case, there is a difference in the nature of the excited-state transitions being probed. Because the ligand participating in the LMCT transition is not the same ligand involved in the initial photon absorption, differences in the corresponding dynamics should not be surprising. Still, it is possible that that solution inhomogeneity becomes a factor on short timescales, producing distinct transients in the SVD analysis that arise from MLCT states involving ligands that have been rendered essentially nonequivalent. This phenomenon is well-known in solid-state spectroscopy, with MLCT energies shifted up to 1000 cm^{-1} between idential ligands on the same metal, owing to variations in their local environments (35, 36).

Fig. 5. Kinetic profile (λ_{probe} = 660 nm) for $Ru(dttb)_3^{2+}$ in aqueous solution following <150 fs excitation at 388 nm.

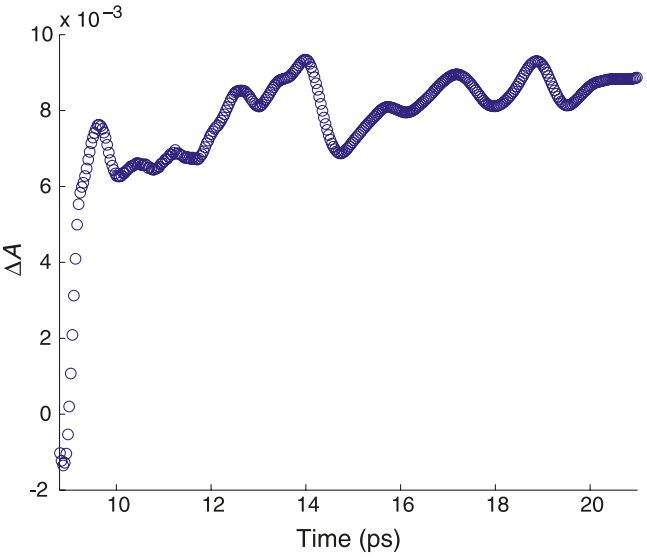

Concluding remarks

Our investigation of a series of related complexes underscores the effect that subtle changes in substituents on the bipyridine ligand have on the early relaxation processes that follow photon absorption. While our investigation produced qualitatively similar transient absorption spectra, the use of SVD revealed subtle differences between the complexes depending on the nature of the ligand. For the complexes where data are available, using longer wavelength excitation, namely $Ru(bpy)_3^{2+}$ and $Ru(dmb)_3^{2+}$, we compared our spectra for 388 nm excitation and noted several kinetic discrepancies, which further underscores the excitation and probe wavelength-dependence in transition metal photophysics. We acknowledge that information is lost within the IRF of our instrument in many cases. However, the pump wavelengths housed in our system allows for the probing of Franck–Condon states at the blue edge of the ^{1}MLCT absorption band as well as ligand-centered transitions, states that have not been probed by the conventional wavelengths used by others. While it is ideal to have data collected at various pump wavelengths, probe windows, and timescales on a single instrument, in reality this is feasible for only a very small portion of the overall timescale for electronic and vibrational relaxation, which can span from microseconds to femtoseconds in solution.

The impetus for using femtosecond absorption spectroscopy to characterize further the early events following photoexcitation of ruthenium(II) polypyridyl complexes was two-fold: (1) the τ = 1–3 ns time constant for luminescence at 500 nm that we measured for various 4,4′-substituted homoleptic complexes warranted further investigation, and (2) our ability to excite samples at both 258 and 388 nm, in conjunction with published transient absorption data collected at additional pump wavelengths for similar species, would begin a systematic investigation of the excitation-dependence of early photophysical events in transition metal complexes. Together with the findings of several other researchers, we anticipate that a detailed investigation of the excitation-wavelength dependence of transition metal complex photophysical parameters will outline a more realistic picture of inorganic photophysics where simple cascade population dynamics are not obeyed.

Acknowledgements

We gratefully acknowledge the Natural Sciences and Engineering Research Council of Canada (NSERC) for financial support of this work and the Canada Foundation for Innovation and the Nova Scotia Research Innovation Trust for research infrastructure. We also thank D. Magde for insightful discussions, P.D. Wentzell for his invaluable help with chemometric analyses and MATLAB®, and A. Thompson for use of her HPLC.

References

1. A. Hagfeldt and M. Gratzel. Acc. Chem. Res. **33**, 269 (2000).
2. J. Badjie, V. Balzani, A. Credi, S. Silvi, and J. Stoddart. Science (Washington, D.C.), **303**, 1845 (2004).
3. P. Mobian, J. Kern, and J. Sauvage. Angew. Chem. **43**, 2392 (2004).
4. M. Venturi, V. Balzani, R. Ballardini, A. Credi, and M. Gandolfi. Int. J. Photoenergy, **6**, 1 (2004).
5. N.H. Damrauer, G. Cerullo, A. Yeh, T.R. Boussie, C.V. Shank, and J.K. McCusker. Science (Washington, D.C.), **275**, 54 (1997).
6. N.H. Damrauer and J.K. McCusker. J. Phys. Chem. A, **103**, 8440 (1999).
7. A.T. Yeh, C.V. Shank, and J.K. McCusker. Science (Washington, D.C.), **289**, 935 (2000).
8. A. Vlcek. Coord. Chem. Rev. **200**, 933 (2000).
9. J. McCusker. Acc. Chem. Res. **36**, 876 (2003).
10. E.A. Juban and J.K. McCusker. J. Am. Chem. Soc. **127**, 6857 (2005).
11. B. Kraabel, J.C. Hummelen, D. Vacar, D. Moses, N. Sariciftci, A. Heeger, and F. Wudl. J. Chem. Phys. **104**, 4267 (1996).
12. C.N. Fleming, K.A. Maxwell, J.M. DeSimone, T.J. Meyer, and J.M. Papanikolas. J. Am. Chem. Soc. **123**, 10336 (2001).
13. I.R. Farrell, P. Matousek, and A. Vlcek, Jr. J. Am. Chem. Soc. **121**, 5296 (1999).
14. I.R. Farrell, P. Matousek, M. Towrie, A. Parker, D. Grills, M. George, and A. Vicek, Jr. Inorg. Chem. **41**, 4318 (2002).
15. C.G. Garcia, J.F. de Lima, and N.Y. Murakami Iha. Coord. Chem. Rev. **196**, 219 (2000).
16. G. Benko, J. Kallioinen, J.E.I. Korppi-Tommola, A.P. Yartsev, and V. Sundstrom. J. Am. Chem. Soc. **124**, 489 (2002).
17. N. Anderson, X. Ai, and T. Lian. J. Phys. Chem. B, **107**, 14414 (2003).
18. G. Benko, J. Kallioinen, P. Myllperkio, P.F. Trif, J.E.I. Korppi-Tommola, A. Yartsev, and V. Sundstrom. J. Phys. Chem. B, **108**, 2862 (2004).
19. R. Bernstein and A. Zewail. J. Phys. Chem. **90**, 3467 (1986).
20. A.J. Nozik. Annu. Rev. Phys. Chem. **52**, 193 (2001).
21. N.J. Turro. Modern molecular photochemistry. University Science Books, Mill Valley, California. 1991.
22. J. Shiang, I. Walker, N. Anderson, A. Cole, and R. Sension. J. Phys. Chem. B, **103**, 10532 (1999).
23. A.C. Bhasikuttan, M. Suzuki, S. Nakeshima, and T. Okada. J. Am. Chem. Soc. **124**, 8398 (2002).
24. S.A. McFarland, F.S. Lee, K. Cheng, F.L. Cozens, and N.P. Schepp. J. Am. Chem. Soc. **127**, 7065 (2005).
25. M. Beer and H. Longuet-Higgins. J. Chem. Phys. **23**, (1955).
26. M. Gutmann, M. Gudipati, P.-F. Schonzart, and G. Hohlneicher. J. Phys. Chem. 2433 (1992).
27. Y. Hirata. J. Phys. Chem. **96**, 6559 (1992).
28. H. Gampp, M. Maeder, C. Meyer, and A. Zuberbühler. Talanta, **33**, 943 (1986).
29. D.G. Lambright, S. Balasubramanian, and S.G. Boxer. Chem. Phys. **158,** 249 (1991).
30. K.N. Walda, X. Liu, V.S. Sharma, and D. Magde. Biochemistry, **33**, 2198 (1994).
31. J. Hofrichter, J.H. Sommer, E.R. Henry, and W.A. Eaton. Proc. Natl. Acad. Sci. U.S.A. **80**, 2235 (1983).
32. S. Yamaguchi and H. Hamaguchi. J. Chem. Phys. **109**, 1397 (1998).
33. A.L. Harris, J.K. Brown, and C.B. Harris. Annu. Rev. Phys. Chem. **39**, 341 (1988).
34. D.A.V. Kliner, J.C. Alfano, and P.F. Barbara. J. Chem. Phys. **98**, 5375 (1993).
35. H. Riesin, Y. Gao, and E. Krausz. Chem. Phys. Lett. **228**, 610 (1994).
36. H. Riesin, Y. Gao, and E. Krausz. Int. Rev. Phys. Chem. **16**, 291 (1997).